Physicochemical Effects on Photocatalytic Water Oxidation by Titanium Fluorooxynitride Powder under Visible Light

Kazuhiko Maeda,[†] Byongjin Lee,[†] Daling Lu,[‡] and Kazunari Domen*,[†]

Department of Chemical System Engineering, The University of Tokyo, 7-3-1 Hongo, Bunkyo-ku, Tokyo 113-8656, Japan, and Center for Advanced Materials Analysis, Tokyo Institute of Technology, 2-12-1 Ookayama, Meguro-ku, Tokyo 152-8550, Japan

Received February 20, 2009. Revised Manuscript Received April 6, 2009

Titanium fluorooxynitride ($TiN_xO_yF_z$) powder prepared by thermal treatment of NH_4TiOF_3 with NH_3 or N_2 is examined as a photocatalyst for water oxidation to form molecular oxygen under visible light ($\lambda > 420$ nm). Nitridation of NH_4TiOF_3 under NH_3 flow at 773 K for durations longer than 0.5 h results in the production of well-crystallized $TiN_xO_yF_z$ particles with an anatase crystal structure and a broad absorption band in the vicinity of 530 nm. The as-prepared materials exhibit good activity for O_2 evolution from aqueous solution under visible light in the presence of silver nitrate as an electron acceptor. Although thermal treatment of NH_4TiOF_3 under N_2 flow in a similar manner also yields $TiN_xO_yF_z$, the as-prepared material exhibits only a small photon absorption shoulder at 400−500 nm consistent with the low nitrogen content of the product. The experimental results indicate that enhanced photocatalytic activity in this system requires suppression of the production of reduced titanium species, which act as electron−hole recombination centers, and the generation of high nitrogen content to obtain a broad response in the visible light band.

1. Introduction

Titanium dioxide (TiO_2) having an anatase or rutile crystal structure has attracted considerable attention as a photocatalytic material in a wide variety of applications, including air purification, decomposition of organic pollutants in aqueous media, and solar energy conversion (water splitting).[1] Despite the superior material properties and low cost of TiO_2, however, its use as a photocatalyst is limited by its relatively large band gap energy (>3 eV), which restricts activity to ultraviolet (UV) wavelengths ($\lambda < 400$ nm). Numerous attempts have been made to modify TiO_2 to utilize visible wavelengths ($\lambda > 400$ nm)[2−5] and to develop new materials that can function efficiently under visible light.[6−11]

Our group has studied anatase-structured titanium fluorooxynitride ($TiN_xO_yF_z$) as a possible photocatalyst for water splitting under visible light.[5] The basic crystal structure of anatase TiO_2 is illustrated schematically in Figure 1.[12] Doping of TiO_2 with nitrogen (TiN_xO_y) has been studied extensively as a means of obtaining a visible-light-responsive photocatalyst. However, photon absorption by this material in the visible region is limited to a shoulder-like absorption band that extends up to 500 nm in addition to the intrinsic absorption band of the host TiO_2 (<400 nm).[4a,5] In contrast, $TiN_xO_yF_z$ has an intense absorption band at approximately 530 nm, making this material more efficient for use in visible-light-driven photochemical reactions. The activity for water oxidation exhibited by $TiN_xO_yF_z$ is 10 times that for TiN_xO_y under visible light.[5] Density functional calculations indicate that the visible-light response of $TiN_xO_yF_z$ is attributable to electron transition from the N 2p doping level above the O 2p valence band to the conduction band formed by empty Ti 3d orbitals.[5b] However, the relationship between the structural characteristics and the photocatalytic performance of $TiN_xO_yF_z$ has yet to be investigated in detail.

Thermal ammonolysis is a convenient technique for synthesizing particulate metal (oxy)nitrides from the corre-

* To whom corresponding author should be addressed. Tel.: +81-3-5841-1148. Fax: +81-3-5841-8838. E-mail: domen@chemsys.t.u-tokyo.ac.jp.
[†] The University of Tokyo.
[‡] Tokyo Institute of Technology.

(1) (a) Hoffmann, M. R.; Martin, S. T.; Choi, W.; Bahnemann, D. W. *Chem. Rev.* **1995**, *95*, 69. (b) Linsebigler, A. L.; Lu, G. Q.; Yates, J. T. *Chem. Rev.* **1995**, *95*, 735. (c) Fujishima, A.; Rao, T. N.; Tryk, D. A. *J. Photochem. Photobiol., C* **2000**, *1*, 1.
(2) (a) Herrmann, J.-M.; Disdier, J.; Pichat, P. *Chem. Phys. Lett.* **1984**, *108*, 618. (b) Kato, H.; Kudo, A. *J. Phys. Chem. B* **2002**, *106*, 5029. (c) Niishiro, R.; Konta, R.; Kato, H.; Chun, W.-J.; Asakura, K.; Kudo, A. *J. Phys. Chem. C* **2007**, *111*, 17420.
(3) O'Regan, B.; Grätzel, M. *Nature (London)* **1991**, *353*, 737.
(4) (a) Asahi, R.; Morikawa, T.; Ohwaki, T.; Aoki, K.; Taga, Y. *Science* **2001**, *293*, 269. (b) Khan, S. U. M.; Al-Shahry, M.; Ingler, W. B., Jr. *Science* **2002**, *297*, 2243. (c) Sakthivel, S.; Kisch, H. *Angew. Chem., Int. Ed.* **2003**, *42*, 4908.
(5) (a) Nukumizu, K.; Nunoshige, J.; Takata, T.; Kondo, J. N.; Hara, M.; Kobayashi, H.; Domen, K. *Chem. Lett.* **2003**, *32*, 196. (b) Maeda, K.; Shimodaira, Y.; Lee, B.; Teramura, K.; Lu, D.; Kobayashi, H.; Domen, K. *J. Phys. Chem. C* **2007**, *111*, 18264.
(6) (a) Maeda, K.; Takata, T.; Hara, M.; Saito, N.; Inoue, Y.; Kobayashi, H.; Domen, K. *J. Am. Chem. Soc.* **2005**, *127*, 8286. (b) Maeda, K.; Teramura, K.; Takata, T.; Hara, M.; Saito, N.; Toda, K.; Inoue, Y.; Kobayashi, H.; Domen, K. *J. Phys. Chem. B* **2005**, *109*, 20504.
(7) (a) Lee, Y.; Terashima, H.; Shimodaira, Y.; Teramura, K.; Hara, M.; Kobayashi, H.; Domen, K.; Yashima, M. *J. Phys. Chem. C* **2007**, *111*, 1042. (b) Lee, Y.; Teramura, K.; Hara, M.; Domen, K. *Chem. Mater.* **2007**, *19*, 2120.
(8) Nakamura, R.; Okamoto, A.; Osawa, H.; Irie, H.; Hashimoto, K. *J. Am. Chem. Soc.* **2007**, *129*, 9596.
(9) Arai, T.; Yanagida, M.; Konishi, Y.; Iwasaki, Y.; Sugihara, H.; Sayama, K. *J. Phys. Chem. C* **2007**, *111*, 7574.
(10) Wang, D.; Kako, T.; Ye, J. *J. Am. Chem. Soc.* **2008**, *130*, 2724.
(11) Abe, R.; Takami, H.; Murakami, N.; Ohtani, B. *J. Am. Chem. Soc.* **2008**, *130*, 2724.
(12) ISCD card no. 44882.

10.1021/cm9005162 CCC: $40.75
Published on Web 05/04/2009

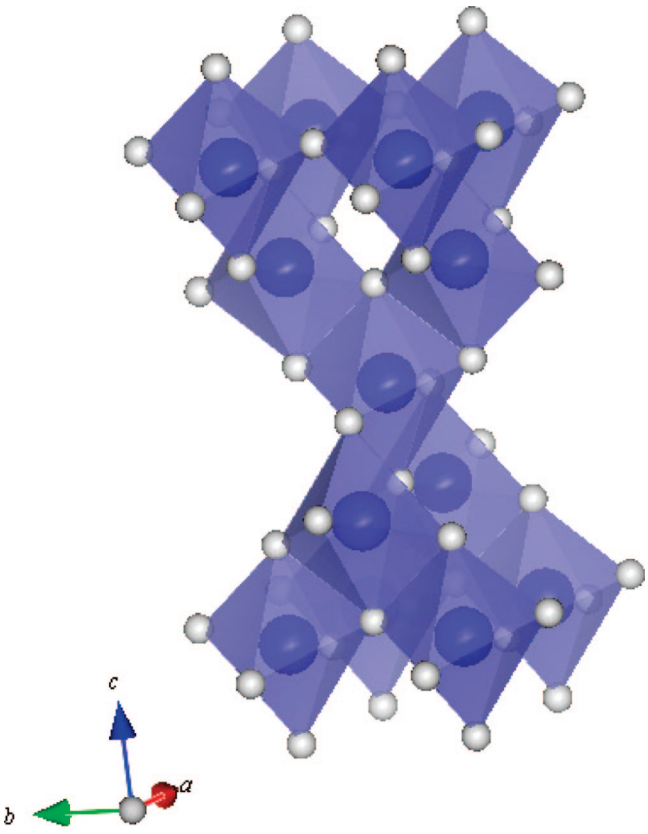

Figure 1. Schematic illustration of crystal structure of anatase TiO_2.

sponding precursor, and the physicochemical properties of the products can be controlled by this approach through appropriate adjustment of the preparation conditions.[6b,7b,13−21] In general, the functionality (e.g., photocatalytic activity) of a given material is strongly dependent on the physicochemical characteristics.[6b,7b,13b,18−21] Therefore, investigating the relationship between the functionality and physicochemical characteristics of a material is of interest and is expected to provide useful information for further refinement of such systems. However, systematic studies of the relationship between the preparation conditions and the physicochemical properties of fluorooxynitrides prepared by thermal ammonolysis have yet to be undertaken so far.

In the present study, the structure−functionality relationship is investigated for $TiN_xO_yF_z$ by preparation of a range of variants exploiting the controllability of thermal ammonolysis. $TiN_xO_yF_z$ is prepared from NH_4TiOF_3 powder by thermal treatment with NH_3 or N_2, and the obtained products are examined as photocatalysts for water oxidation under visible light ($\lambda > 420$ nm). The relationship between the physicochemical properties and the catalytic performance of the material is then discussed on the basis of the physicochemical analyses.

2. Experimental Section

2.1. Materials and Reagents. The precursor NH_4TiOF_3 employed for preparation of $TiN_xO_yF_z$ was synthesized from aqueous H_3BO_4 solution with the addition of $(NH_4)_2TiF_6$ by a modified liquid-phase deposition method.[22] Details of the procedure have been reported previously.[5b] The as-prepared material was confirmed by X-ray diffraction (XRD) measurement to consist of a single NH_4TiOF_3 phase.

$TiN_xO_yF_z$ was prepared by heating the as-prepared NH_4TiOF_3 at 773 K under NH_3 or N_2 flow using a quartz reactor. To investigate the effect of preparation parameters, nitridation time and flow rate were varied from 0.5 to 10 h and from 50 to 500 $mL \cdot min^{-1}$, respectively. To prevent oxygen contamination,[5a] the NH_4TiOF_3 precursor (0.50 g) was wrapped with nickel mesh and set at the center of a nickel tube inside the quartz reactor. After heating for a given period, the sample was cooled to room temperature under continuous gas flow.

2.2. Characterization of Catalysts. The prepared samples were studied by powder XRD (RINT-2100, Rigaku; Cu Kα), scanning electron microscopy (SEM; S-4700, Hitachi), and UV−visible diffuse reflectance spectroscopy (DRS; V-560, Jasco). The Brunauer−Emmett−Teller (BET) surface area was measured using a Coulter SA-3100 instrument at liquid nitrogen temperature. The amount of nitrogen and fluorine in the sample was determined by elemental analysis (CHNS-932, LECO, and SX-Elements Micro Analyzer YS-10, Yanaco).

2.3. Photocatalytic Reactions. Reactions were carried out in a Pyrex top-irradiation reaction vessel connected to a closed gas circulation system. Photooxidation of H_2O into O_2 was performed in aqueous solution containing silver nitrate (0.01 M) as a sacrificial electron acceptor. Into this aqueous solution were dispersed 0.1 g of the $TiN_xO_yF_z$ photocatalyst and 0.2 g of La_2O_3 powder (a basic metal oxide) to buffer the pH of the reactant solution to 8−9 during the reaction.[5,18a,19] The reactant solution was evacuated several times to remove air completely prior to irradiation under a 300 W xenon lamp fitted with a cutoff filter to block UV light ($\lambda > 420$ nm). The reactant solution was maintained at room temperature by a flow of cooling water during the reaction. The evolved gases were analyzed by gas chromatography.

3. Results and Discussion

3.1. Effect of Nitridation Time. The parameters of ammonolysis, including temperature, time, and gas flow rate, vary the reactivity of NH_3 toward the solid material, leading to marked dissimilarities among the final products.[6b,7b,13−21] In the present study, the nitridation temperature was fixed at 773 K. Preparation at higher or lower temperatures was found in preliminary experiments to be unsuccessful because of the production of $TiOF_2$ as an impurity at 723 K and at higher temperatures because of reduced product yield associated with the formation of reduced titanium species that can act as electron−hole recombination centers.

(13) (a) Johnson, W. C. *J. Am. Chem. Soc.* **1930**, *52*, 5160. (b) Maeda, K.; Saito, N.; Inoue, Y.; Domen, K. *Chem. Mater.* **2007**, *19*, 4092.
(14) Tessier, F.; Marchand, R. *J. Alloys Compd.* **1997**, *410*, 262.
(15) Tessier, F.; Marchand, R.; Laurent, Y. *J. Eur. Ceram. Soc.* **1997**, *17*, 1825.
(16) Marchand, R.; Tessier, F.; DiSalvo, F. J. *J. Mater. Chem.* **1999**, *9*, 297.
(17) Schwenzer, B.; Loeffler, L.; Seshadri, R.; Keller, S.; Lange, F. F.; DenBaars, S. P.; Mishra, U. K. *J. Mater. Chem.* **2004**, *14*, 637.
(18) (a) Hitoki, G.; Ishikawa, A.; Takata, T.; Kondo, J. N.; Hara, M.; Domen, K. *Chem. Lett.* **2002**, *31*, 736. (b) Hara, M.; Hitoki, G.; Takata, T.; Kondo, J. N.; Kobayashi, H.; Domen, K. *Catal. Today* **2003**, *78*, 555.
(19) Kasahara, A.; Nukumizu, K.; Takata, T.; Kondo, J. N.; Hara, M.; Kobayashi, H.; Domen, K. *J. Phys. Chem. B* **2003**, *107*, 791.
(20) Schwenzer, B.; Hu, J.; Seshadri, R.; Keller, S.; DenBaars, S. P.; Mishra, U. K. *Chem. Mater.* **2004**, *16*, 5088.
(21) Hisatomi, T.; Teramura, K.; Kubota, J.; Domen, K. *Bull. Chem. Soc. Jpn.* **2008**, *81*, 1647.
(22) Deki, S.; Aoi, Y.; Hiroi, O.; Kajinami, A. *Chem. Lett.* **1996**, *25*, 433.

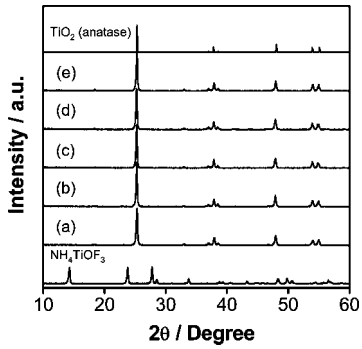

Figure 2. Powder XRD patterns of samples obtained by nitriding NH_4TiOF_3 under NH_3 flow (250 mL·min^{-1}) at 773 K for (a) 0.5, (b) 1, (c) 3, (d) 5, and (e) 10 h. Data for NH_4TiOF_3 and anatase TiO_2 (ICSD card no. 44882) are also shown.

Table 1. Elemental Analyses for Samples Prepared by Nitriding NH_4TiOF_3 at 773 K under NH_3 Flow (250 mL·min^{-1}) for Various Nitridation Times

	elemental content, wt %		atomic ratio		
nitridation time, h	N	F	N/Ti	O/Ti	F/Ti
0			1	1	3
0.5	1.83	3.56	0.056	1.877	0.080
1	1.66	3.52	0.053	1.880	0.082
3	1.87	2.26	0.056	1.890	0.050
5	1.83	2.03	0.056	1.893	0.046
10	1.83	2.04	0.056	1.893	0.046

Figure 2 shows the powder XRD patterns of samples obtained by nitriding NH_4TiOF_3 at 773 K under NH_3 flow (250 mL·min^{-1}) for several periods, along with those for the NH_4TiOF_3 precursor and anatase TiO_2.[12] The crystal structure of the prepared samples can be assigned to anatase similar to TiO_2, regardless of nitridation time. No peaks assignable to NH_4TiOF_3 are present in the XRD pattern, indicating complete nitridation of the NH_4TiOF_3 precursor under the present nitridation conditions, although one unidentified peak with negligible diffraction intensity can be identified at $2\theta = 33.0°$. The intensity of the diffraction peaks assigned to the anatase phase increased slightly with nitridation time from 0.5 to 1.0 h, but prolonged nitridation had little further effect on the diffraction pattern of the nitrided product.

Table 1 lists the atomic ratios of N/Ti, O/Ti, and F/Ti for the same set of samples. The N/Ti and F/Ti ratios were measured by elemental analyses, whereas the O/Ti ratio was estimated on the basis of the nitrogen and fluorine content in the sample as determined by elemental analyses and the charge balance among Ti^{4+}, N^{3-}, O^{2-}, and F^- assuming charge balance among these ions and no vacancies or interstitial atoms.[23] The N/F ratio in the samples deviates slightly from unity, indicating that the obtained samples contain defect sites. Nevertheless, the results of XRD and elemental analyses confirm the production of nearly single-phase $TiN_xO_yF_z$. With increasing nitridation time, the F/Ti ratio tends to decrease, while the N/Ti remains almost constant. Assuming that all titanium species in NH_4TiOF_3 (0.50 g) are converted to $TiN_xO_yF_z$ upon nitridation, the yield of the nitridation product should be approximately 0.29 g. However, the actual yields were on the order of 0.18 g, regardless of nitridation conditions, which is considerable below the expected value. This result suggests that part of the NH_4TiOF_3 precursor was decomposed in the preparation process to form volatile TiF_4, which would have sublimated during nitridation.[24] This behavior is supported by the high O/Ti ratio of the present samples compared to that of the NH_4TiOF_3 precursor, despite the absence of another oxygen source in the reactor.

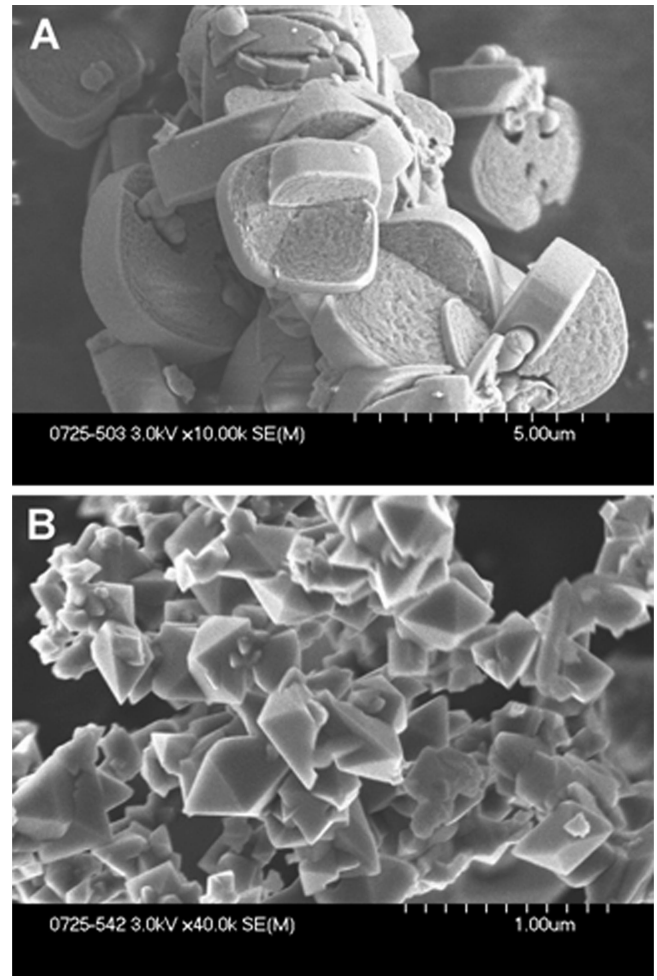

Figure 3. SEM images of (A) NH_4TiOF_3 and (B) $TiN_xO_yF_z$ prepared by nitriding NH_4TiOF_3 under NH_3 flow (250 mL·min^{-1}) at 773 K for 1 h.

Figure 3 shows SEM images of NH_4TiOF_3 samples before and after nitridation. The NH_4TiOF_3 particles are micrometer-scale aggregates of primary particles forming a wheel-like arrangement. Upon nitridation, the characteristic shape of NH_4TiOF_3 undergoes a marked change to afford octahedral-shaped particles, accompanied by the compositional change to $TiN_xO_yF_z$. A TEM image and electron diffraction pattern of a $TiN_xO_yF_z$ sample are shown in Figure 4. The distinct lattice fringe and electron diffraction pattern, in addition to the sharp edges and planes observed in the SEM image, indicate that the $TiN_xO_yF_z$ is highly crystalline. As expected

(23) Elemental analyses showed that no hydrogen could be detected in the prepared samples. In addition, our previous study using X-ray absorption spectroscopy has revealed that the electric state of titanium in $TiN_xO_yF_z$ is very close to that in anatase TiO_2; that is, the oxidation number is almost +4 (ref 5b). One can therefore calculate the chemical composition considering the charge balance of the constituent elements.

(24) Lide, D. R. *Handbook of Chemistry and Physics*, 83rd ed.; CRC Press: Boca Raton, FL, 2002.

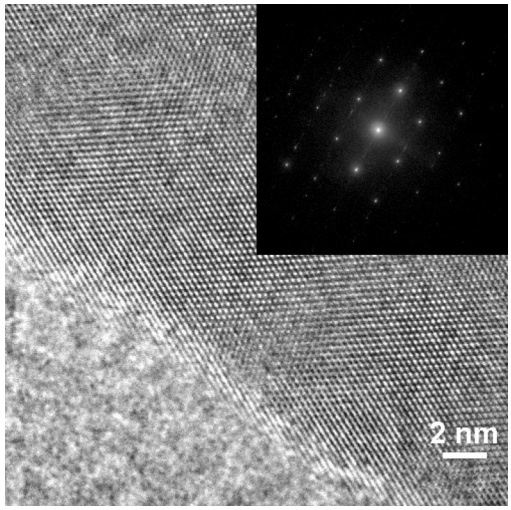

Figure 4. TEM image and electron diffraction pattern of $TiN_xO_yF_z$ prepared by nitriding NH_4TiOF_3 under NH_3 flow (250 mL·min^{-1}) at 773 K for 1 h.

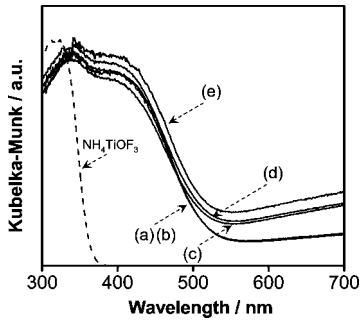

Figure 5. UV−visible diffuse reflectance spectra for samples obtained by nitriding NH_4TiOF_3 under NH_3 flow (250 mL·min^{-1}) at 773 K for (a) 0.5, (b) 1, (c) 3, (d) 5, and (e) 10 h. Data for NH_4TiOF_3 and anatase TiO_2 (ICSD card no. 44882) are also shown.

from the results of XRD analyses, however, there are no noticeable differences in surface morphology among the samples prepared under the various nitridation conditions. The specific surface area is typically approximately 10 m^2·g^{-1}.

Figure 5 shows the UV−visible diffuse reflectance spectra for samples obtained by nitriding NH_4TiOF_3 at 773 K under NH_3 flow (250 mL·min^{-1}) for several periods. All samples display a wide absorption band in the visible region, although an absorption band assignable to the band gap transition of anatase TiO_2 prevails marginally at approximately 380 nm. As reported previously, the visible light response of $TiN_xO_yF_z$ originates from the transition from the doping level formed by the N 2p orbitals in the forbidden band (located above the valence band consisting of O 2p orbitals) to the conduction band (consisting of empty Ti 3d orbitals).[5b] The absorption at wavelengths longer than 600 nm, attributable to reduced titanium species (e.g., Ti^{3+}) accompanied by defect sites[5b,19,21] strengthens with reaction time, indicating that prolonged nitridation results in the reduction of Ti^{4+} species in $TiN_xO_yF_z$. An essentially identical tendency has been reported previously for $LaTiO_2N$[19] and $Zn_xTiO_yN_z$.[21] The presence of Ti^{3+} species in $TiN_xO_yF_z$ seems to contradict the result of X-ray absorption spectroscopy, which has revealed that the oxidation number of titanium in $TiN_xO_yF_z$ is close to +4.[5b] This discrepancy is probably attributed to the difference in sensitivity between X-ray spectroscopy and UV−visible spectroscopy, and the amount of the reduced titanium species (Ti^{3+}) is considered to be very low, as compared to the main Ti^{4+} species.

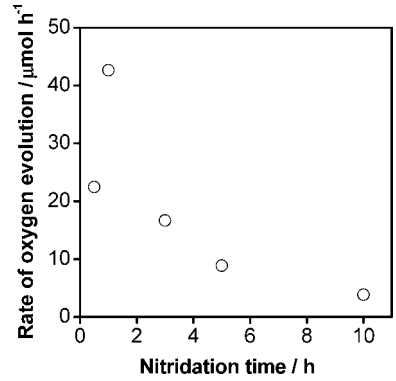

Figure 6. Dependence of rate of O_2 evolution by $TiN_xO_yF_z$ on nitridation time of NH_4TiOF_3. Reaction conditions: catalyst, 0.1 g; La_2O_3, 0.2 g; aqueous silver nitrate solution, 0.01 M, 200 mL; light source, xenon lamp (300 W) with cutoff filter; reaction vessel, Pyrex top-irradiation type.

On the basis of these results, nitridation for extended periods appears to lead to the generation of reduced titanium species (defect sites) in $TiN_xO_yF_z$, while the structural properties remain little changed. The production of defect sites is expected to affect the photocatalytic activity of $TiN_xO_yF_z$. The effect of extended nitridation on photocatalytic performance is shown in Figure 6. Consistent with previous reports, the activity for O_2 evolution decreases gradually with reaction time,[5] primarily attributable to the deposition of metallic silver on the catalyst surface, which blocks light absorption and obstructs active sites. All of the present samples display activity for O_2 evolution. However, the rate of O_2 evolution increases with the nitridation time employed in the preparation of the catalyst up to a maximum evolution rate at 1 h nitridation, beyond which the activity of the samples begins to decrease markedly. In the initial stage of the reaction, a negligible amount of evolved N_2 was detected in all cases. However, continuous N_2 evolution was not observed, confirming the stability of $TiN_xO_yF_z$ as a photocatalyst for water oxidation.[5b]

3.2. Effect of Ammonia Flow Rate. Variation of the NH_3 flow rate from 50 to 500 mL·min^{-1} in ammonolysis at 773 K for 1 h was found not to result in appreciable changes in the crystal phase of the nitrided products. As shown in Figure 7, there are no noticeable changes in the XRD patterns except for a slight weakening of peak intensity between the samples prepared at flow rates of 250 and 500 mL·min^{-1}. It should be noted that the production of a single-phase anatase structure was also achieved by heating NH_4TiOF_3 under N_2 flow in a similar manner. The particles of the N_2-treated sample are granular aggregates consisting of primary particles of 50−100 nm in size (see Supporting Information, Figure S1), which are smaller than the aggregates formed by NH_3 treatment (100−400 nm). The XRD analyses, however, show that the intensity of diffraction peaks for the sample prepared using N_2 is stronger than for the samples prepared using NH_3. Previous X-ray analyses have revealed that the partial substitution of N^{3-} and F^- at the O^{2-} site in the octahedral

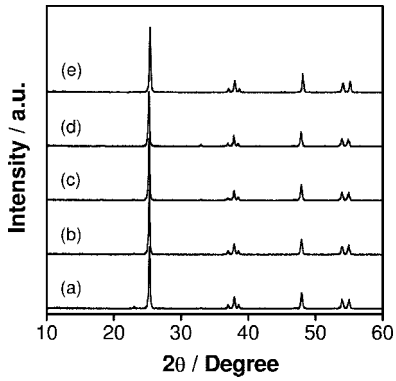

Figure 7. Powder XRD patterns of samples obtained by nitriding NH_4TiOF_3 at 773 K for 1 h under NH_3 flow at (a) 50, (b) 100, (c) 250, and (d) 500 mL·min^{-1} and (e) N_2 flow at 100 mL·min^{-1}.

Table 2. Elemental Analyses for Samples Prepared by Nitriding NH_4TiOF_3 at 773 K for 1 h under Various Gas Flow Rates

flow conditions		amount of elements, wt %		atomic ratio		
rate, mL·min^{-1}	gas	N	F	N/Ti	O/Ti	F/Ti
50	NH_3	1.09	4.38	0.041	1.879	0.120
100		1.32	3.98	0.046	1.880	0.102
250		1.66	3.52	0.053	1.880	0.082
500		2.07	2.67	0.059	1.883	0.057
100	N_2	0.08	2.03	0.004	1.953	0.082

TiO_6 unit of anatase TiO_2 results in slight distortion of the crystal lattice, reducing the uniformity of the lattice.[5b] It is therefore considered that the relatively low degree of anion substitution in the sample prepared using N_2 results in less loss of uniformity in the anatase crystal lattice, contributing to the stronger diffraction peak intensity compared to the samples prepared using NH_3.

Table 2 lists the atomic ratios of N/Ti, O/Ti, and F/Ti for these samples. Both nitrogen and fluorine are present in all samples, indicating that all of the products are $TiN_xO_yF_z$ with the anatase crystal structure. The N/F ratio in these samples deviates slightly from unity, indicating that the obtained samples contain defect sites. With increasing NH_3 flow rate, the N/Ti ratio tends to increase while the F/Ti ratio decreases. It has been reported that increasing NH_3 flow rate at a given nitridation temperature and time contributes to an increase in reactivity of NH_3 with the solid surface, promoting the generation of nitrided products.[18b,25] The results for the present $TiN_xO_yF_z$ system are in good agreement with this principle. In contrast, the nitrogen content in $TiN_xO_yF_z$ prepared under N_2 flow is at least an order of magnitude lower than that for samples prepared using NH_3. As the NH_4TiOF_3 precursor contains nitrogen as a principal component and the nitrogen molecules are not activated at the present nitridation temperature (773 K), the remaining nitrogen in the sample prepared under N_2 flow should be derived from the precursor. It was thus found that $TiN_xO_yF_z$ can be prepared even without using NH_3 as a reactant gas, although the use of NH_3 gas is indispensable for the synthesis of $TiN_xO_yF_z$ with higher nitrogen content.

Diffuse reflectance spectra for the same set of samples are shown in Figure 8. The observed variation among samples is similar to that for samples prepared using different

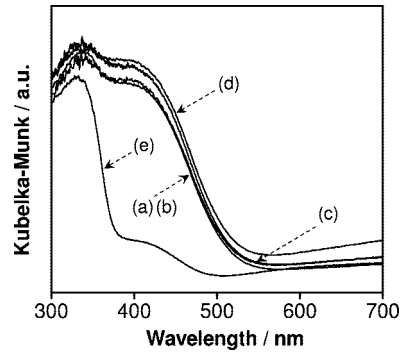

Figure 8. UV−visible diffuse reflectance spectra for samples obtained by nitriding NH_4TiOF_3 at 773 K for 1 h under NH_3 flow at (a) 50, (b) 100, (c) 250, and (d) 500 mL·min^{-1} and (e) N_2 flow at 100 mL·min^{-1}.

Table 3. Dependence of Flow Conditions on Activity[a]

flow condition		
rate, mL·min^{-1}	gas	activity, μmol h^{-1}
50	NH_3	34.9
100		38.2
250		42.6
500		19.2
100	N_2	1.7

[a] Reaction conditions: catalyst, 0.1 g; La_2O_3, 0.2 g; aqueous silver nitrate solution, 0.01 M, 200 mL; light source, xenon lamp (300 W) with cutoff filter; reaction vessel, Pyrex top-irradiation type.

nitridation times (Figure 5). That is, the absorption band at wavelengths longer than 600 nm, assigned to reduced titanium species, becomes more pronounced as the rate of NH_3 flow increases. This result is reasonable considering the increasing nitridation ability of NH_3 with increasing flow rate at a given temperature and for a given time. The use of N_2 as a reactant gas does not result in the appearance of a broad absorption band, producing only the shoulder-like absorption at 400−500 nm in addition to the intrinsic absorption band of TiO_2 and the background absorption above 600 nm. This relatively weak absorption profile is similar to that of TiN_xO_y[4a,5b] and appears to originate primarily from the low nitrogen content in the material (see Table 2).

Table 3 lists the photocatalytic activities of $TiN_xO_yF_z$ prepared at various flow rates. All samples photocatalyze visible-light-driven O_2 evolution from aqueous silver nitrate solution. The activity of the samples increases gradually with the NH_3 flow rate employed in preparation to a maximum at 250 mL·min^{-1}. The sample prepared using N_2 gas also exhibits activity for this reaction, although the activity is an order of magnitude lower than that achieved by other samples. The flow conditions of nitridation thus have a substantial impact on the activity of $TiN_xO_yF_z$ for water oxidation.

3.3. Factors Affecting Photocatalytic Activity. As shown in Figure 6, the photocatalytic activity was found to be strongly dependent on the nitridation time employed in the preparation of $TiN_xO_yF_z$. Nitridation for 0.5 to 1.0 h, despite resulting in a doubling of activity, was not found to produce changes in structure, composition, or absorption profile, and the intensity of the XRD peaks increase only slightly over this interval (Figure 2). The change in XRD pattern is very small, and the causative changes could not

(25) Katsura, M. *J. Alloys Compd.* **1992**, *182*, 91.

be readily discerned by SEM. However, the increase in peak intensity suggests an increase in the uniformity of crystallization of $TiN_xO_yF_z$, which could improve the mobility of photogenerated carriers and lead to an enhancement of photocatalytic activity. Nitridation for longer than 1 h resulted in a marked decrease in activity, attributable to the generation of reduced titanium species (Figure 5) that can act as electron−hole recombination centers. It has been shown for certain (oxy)nitrides that suppressing the generation of reduced principal cation species (defect sites) is essential for enhancing photocatalytic activity.[13b,26]

The flow condition was also found to be an important factor contributing to the enhancement of catalytic activity. With increasing NH_3 flow rate from 50 to 250 mL·min^{-1}, the activity gradually improved (Table 3), even though the background absorption assignable to defect sites also increased (Figure 8). This enhancement in activity might be due to the increase in nitrogen content. Kudo et al. reported that rutile TiO_2 doped with rhodium and antimony (TiO_2:Rh/Sb) functions as an active photocatalyst for O_2 evolution from aqueous silver nitrate solution under visible light.[2c] According to that study, the doped Rh^{3+} ions interact with each other at the high doping level to form a sub-band above the O 2p valence band, resulting in the formation of O_2 evolution sites that oxidize water by a four-electron process. Previous density functional calculations have revealed that nitrogen species in $TiN_xO_yF_z$ produce doping levels in the forbidden band above the O 2p valence band and that these levels are responsible for the visible-light photocatalytic activity.[5b] It is therefore considered that the increased nitrogen content is advantageous for the generation of active sites for water oxidation, as in the case of the Rh^{3+} dopant in TiO_2:Rh/Sb photocatalysts.[2c] The drop in activity from 250 to 500 mL·min^{-1} NH_3 is then attributable to the increased generation of defects, as indicated by the diffuse reflectance spectra (Figure 8). The effect of the increased defect density would conceal the positive effect provided by the increased nitrogen content, resulting in a reduction of activity. Despite the relatively small particle size (Figure S1, Supporting Information) and weak background absorption level (Figure 8), the sample prepared using N_2 displayed the lowest activity among the samples examined (Table 3). This low activity is considered to be due to both the poor visible-light-absorption properties (Figure 8) and the low nitrogen content (Table 3), as found for TiN_xO_y in previous research.[5b]

(26) Maeda, K.; Terashima, H.; Kase, K.; Higashi, M.; Tabata, M.; Domen, K. *Bull. Chem. Soc. Jpn.* **2008**, *81*, 927.

4. Conclusions

$TiN_xO_yF_z$ having an anatase crystal structure was successfully prepared by heating NH_4TiOF_3 at 773 K for longer than 0.5 h under NH_3 flow and was demonstrated to be photocatalytically active for the oxidation of water under visible light. The activity of $TiN_xO_yF_z$ for this reaction was shown to be dependent on the nitrogen content and the density of defects in the material. Although $TiN_xO_yF_z$ can be prepared from NH_4TiOF_3 using N_2, the use of NH_3 as a reactant gas is concluded to be indispensable to preparing $TiN_xO_yF_z$ with a broad absorption band in the visible region and high photocatalytic activity for the water oxidation reaction. The use of appropriate parameters in preparation is therefore very important.

Acknowledgment. This work was supported by the Research and Development in a New Interdisciplinary Field Based on Nanotechnology and Materials Science program of the Ministry of Education, Culture, Sports, Science and Technology (MEXT) of Japan. Acknowledgement is extended to the Tokyo Metropolitan Collaboration of Regional Entities for the Advancement of Technological Excellence, Japan Science and Technology Agency (JST).

Supporting Information Available: SEM image of the sample obtained by nitriding NH_4TiOF_3 at 773 K for 1 h under N_2 flow at 100 mL·min^{-1}. This material is available free of charge via the Internet at http://pubs.acs.org.

CM9005162